Myeloid cells from Langerhans cell histiocytosis patients exhibit increased vesicle trafficking and an altered secretome capable of activating NK cells

Daniel W. Hagey,[1,2] Egle Kvedaraite,[2-4+] Mira Akber,[3+] André Görgens,[1,5] Joman Javadi,[1] Tatiana von Bahr Greenwood,[2,6] Caroline Björklund,[7] Selma Olsson Åkefeldt,[2,8] Tova Hannegård-Hamrin,[9,10] Henrik Arnell,[11,12] Katalin Dobra,[1] Nikolas Herold,[2,6] Mattias Svensson,[3] Samir El Andaloussi,[1] Jan-Inge Henter[2,6] and Magda Lourda[2,3]

[1]Department of Laboratory Medicine, Karolinska Institutet, Stockholm, Sweden; [2]Childhood Cancer Research Unit, Department of Women's and Children's Health, Karolinska Institutet, Stockholm, Sweden; [3]Center for Infectious Medicine, Department of Medicine Huddinge, Karolinska Institutet, Karolinska University Hospital, Stockholm, Sweden; [4]Department of Clinical Pathology and Cancer Diagnostics, Karolinska University Hospital, Stockholm, Sweden; [5]Institute for Transfusion Medicine, University Hospital Essen, Essen, Germany; [6]Pediatric Oncology, Astrid Lindgren Children's Hospital, Karolinska University Hospital, Stockholm, Sweden; [7]Department of Pediatric Hematology and Oncology, Umeå University Hospital, Umeå, Sweden; [8]Theme of Children's Health, Karolinska University Hospital, Stockholm, Sweden; [9]Department of Physiology and Pharmacology, Karolinska Institutet, Stockholm, Sweden; [10]Department of Pediatric Anesthesia and Intensive Care, Karolinska University Hospital, Stockholm, Sweden; [11]Pediatric Gastroenterology, Hepatology and Nutrition, Astrid Lindgren Children's Hospital, Karolinska University Hospital, Stockholm, Sweden and [12]Department of Women's and Children's Health, Karolinska Institutet, Stockholm, Sweden

[+]EK and MA contributed equally to this work.

Correspondence: D. Hagey
daniel.hagey@ki.se

M. Lourda
magdalini.lourda@ki.se

Received: January 4, 2023.
Accepted: March 9, 2023.
Early view: March 16, 2023.

https://doi.org/10.3324/haematol.2022.282638

Abstract

Langerhans cell histiocytosis (LCH) is a potentially life-threatening inflammatory myeloid neoplasia linked to pediatric neurodegeneration, whereby transformed LCH cells form agglomerated lesions in various organs. Although MAP-kinase pathway mutations have been identified in LCH cells, the functional consequences of these mutations and the mechanisms that cause the pathogenic behavior of LCH cells are not well understood. In our study, we used an *in vitro* differentiation system and RNA-sequencing to compare monocyte-derived dendritic cells from LCH patients to those derived from healthy controls or patients with Crohn's disease, a non-histiocytic inflammatory disease. We observed that interferon-γ treatment exacerbated intrinsic differences between LCH patient and control cells, including strikingly increased endo- and exocytosis gene activity in LCH patients. We validated these transcriptional patterns in lesions and functionally confirmed that LCH cells exhibited increased endo- and exocytosis. Furthermore, RNA-sequencing of extracellular vesicles revealed the enrichment of pathological transcripts involved in cell adhesion, MAP-kinase pathway, vesicle trafficking and T-cell activation in LCH patients. Thus, we tested the effect of the LCH secretome on lymphocyte activity and found significant activation of NK cells. These findings implicate extracellular vesicles in the pathology of LCH for the first time, in line with their established roles in the formation of various other tumor niches. Thus, we describe novel traits of LCH patient cells and suggest a pathogenic mechanism of potential therapeutic and diagnostic importance.

Introduction

Langerhans cell histiocytosis (LCH) is characterized by the accumulation of langerin[+]CD1a[+] myeloid cells (LCH cells) together with other immune cell populations in inflammatory lesions, which can be fatal or result in a diversity of long-term consequences, including neurodegeneration.[1] The molecular characteristics of LCH began to be understood when it was discovered that most lesions are affected by constitutively activated extracellular signal-regulated kinases (ERK) due to somatic mutations in proteins of the mitogen-activated protein kinase (MAPK) pathway.[1-3] In addition, *BRAF* V600E mutation in LCH patients was found to correlate with a suppressive tumor im-

mune microenvironment and reduced disease-free survival.[4] However, the underlying causes of LCH and the behavior of lesional cells remain elusive.

While research on immune stimulation has previously focused on soluble protein factors, such as cytokines,[5-10] the role of extracellular vesicles (EV) in intercellular communication has only recently been described. EV are 30 nm to 1 μm in size and are secreted in a programmed fashion from the cell surface and endosomal system of all cells.[11] They have been demonstrated to transport lipids, proteins and nucleic acids between cells to influence various processes, including tumor growth.[12] EV can promote phenotypic changes in recipient cells by transferring oncoproteins that activate downstream signaling pathways, such as the MAPK or PI3K–AKT–mTOR, which makes them potential mediators of LCH pathology.[13] However, neither abnormal vesicle trafficking nor EV have previously been investigated in LCH.

In this work, we have utilized an *in vitro* differentiation system[14] to generate mature monocyte-derived dendritic cells (moDC) from blood monocytes of LCH patients and compare them to healthy controls or patients with Crohn's disease (CD), a non-histiocytic inflammatory disease often presenting with granulomas. RNA-sequencing (RNA-seq) of these cells confirmed previously described aspects of LCH and revealed starkly increased levels of various membrane trafficking genes in LCH. We confirmed these expression profiles in lesions and performed functional analyses demonstrating that LCH cells displayed increased endocytosis, reacted specifically to interferon-γ (INFγ) treatment and secreted higher numbers of EV. Interestingly, LCH EV were associated with an enrichment of transcripts involved in cell adhesion, MAPK signaling, T-cell activation and vesicle trafficking, particularly in patients with active LCH. By treating lymphocytes with LCH secretome, a marked increase in the frequency of activated NK cells was observed. Together, these results point to novel mechanisms of LCH pathogenesis that may help to better understand the disease and provide potential therapeutic and diagnostic targets.

Methods

Blood samples

The study cohort includes nine children with a definitive LCH diagnosis (2 sampled twice) that had been cared for in the Karolinska University Hospital (n=8) or Umeå University Hospital (n=1) in Sweden (*Online Supplementary Table S1*) and three children with a definitive CD diagnosis (2 sampled at diagnosis and 1 at follow-up) that had been cared for in the Karolinska University Hospital. Blood samples from healthy controls (n=16) were received from the Clinical immunology and transfusion medicine laboratory (n=11, adults) or the Department of Pediatric Anesthesia and Intensive Care in Karolinska University Hospital (n=5, children). All samples were received after signed informed consent. The study was performed in accordance with the Declaration of Helsinki and approved by the Ethical Review Board in Stockholm.

Isolation of peripheral blood mononuclear cells and purification of monocytes

Peripheral blood mononuclear cells (PBMC) were retrieved after separation of the blood components with Lymphoprep (Axis-Shield PoC AS, Oslo, Norway) and the monocytes were negatively selected using the EasySep™ Human Monocyte Enrichment Kit without CD16 Depletion (STEMCELL Technologies, UK) according to the manufacturer's instructions. The purity of the enriched monocytes was evaluated with flow cytometry[5] and was >90%.

Monocyte differentiation to monocyte-derived dendritic cells

Purified monocytes were seeded at a concentration of 1 million cells/mL in RPMI 1640 medium (Thermo Fischer Scientific, South Logan, US), supplemented with 10% heat-inactivated fetal calf serum (FCS; Sigma-Aldrich, St. Louis, USA), 2 mM L-glutamine (Thermo Fischer Scientific), 10 mM Hepes (N-2-hydroxyethylpiperazine-N-2-ethanesulfonic acid; Thermo Fischer Scientific), 50 ng/mL GM-CSF (PeproTech, New Jersey, USA) and 10 ng/mL IL-4 (PeproTech) for 6 days to achieve differentiation to moDC.

Monocyte-derived dendritic cell stimulation

moDC on day 6 were counted and replated in 6-well plates (1 million cells/mL) in RPMI 1640 medium, supplemented with 10% heat-inactivated FCS, 2 mM L-glutamine, 10 mM Hepes, 50 ng/mL GM-CSF and 10 ng/mL IL-4 ± 2 ng/mL INFγ (PeproTech) for 7 additional days. Mature moDC and culture medium were collected on day 13 and further processed for RNA-seq or transmission electron microscopy (EM) imaging.

RNA-sequencing

RNA from cells or EV was extracted[15] and precipitated as previously described[16] and further explained in the *Online Supplementary Appendix*.

Statistical analysis

GraphPad Prism version 9, Excel, R prcomp and DESeq2 were used to analyze the data as described in the Figure legends. The statistical tests used in each graph and the *P* values are indicated in the figures: **P*<0.05, ***P*<0.01, ****P*<0.001 or *****P*<0.0001. All violin plots were generated in R using ggplot2, with sample mean shown as a large solid dot, standard error as a vertical line and individual data points as rings.

Additional methods used are available in the *Online Supplementary Appendix*.

Results

RNA-sequencing of monocyte-derived dendritic cells

In order to better understand the functional characteristics of the myeloid compartment in LCH, we sought to characterize the intrinsic differences between moDC from LCH patients and healthy controls. In order to accomplish this, we isolated circulating monocytes from three LCH patients (*Online Supplementary Table S1*) and three healthy controls and differentiated them towards immature moDC using a well-established protocol[14,17,18] (Figure 1A). After 7 additional days in culture, the morphology of the cells was studied with EM (Figure 1B) and RNA was extracted for sequencing.

In agreement with previous work,[19] EM visualization of the moDC revealed no substantial differences in their morphological phenotype (Figure 1B). Analysis of RNA-seq data confirmed the purity of the analyzed cells, as the cultures

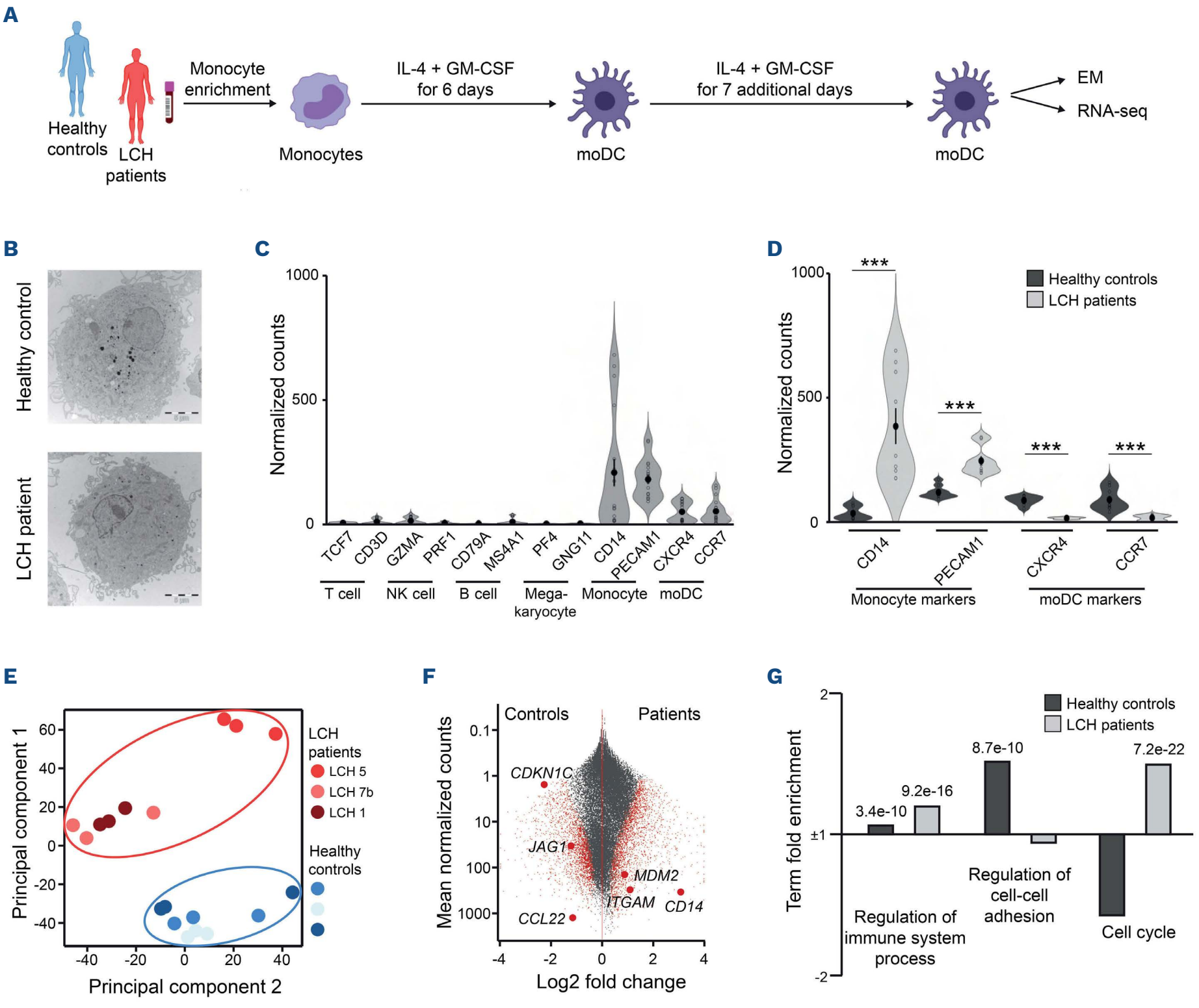

Figure 1. *In vitro* differentiation of monocytes. (A) Schematic diagram of the differentiation protocol applied to monocytes isolated from healthy controls or Langerhans cell histiocytosis (LCH) patients. (B) Electron microscopy (EM) images of control and patient monocyte-derived dendritic cells (moDC). Scale bars are inset. (C) Expression of marker genes for different immune cell populations in all moDC transcriptome data sets. (D) Comparison between control and patient moDC expression of monocyte and moDC genes. ***DESeq2 adjusted *P*<0.001. (E) Principal component analysis of control and patient transcriptomes. (F) Gene expression comparison between control and patient moDC. Illustrative genes found differentially expressed in Allen *et al.*[20] are highlighted. (G) Gene ontology term fold enrichments for genes differentially expressed between control and patient moDC. *P* values for significantly enriched terms are inset. GM-CSF: granulocyte-macrophage colony-stimulating factor.

were enriched in markers of monocytes and DC over those of other immune cells (Figure 1C). In order to see if this pattern was equally true in patient and control cells, we investigated the levels of monocyte and DC markers separately in each group. Interestingly, this revealed that the expression of monocyte genes (e.g., *CD14, PECAM1*) was significantly higher in patients, while the expression of DC markers (e.g., *CXCR4, CCR7*) was significantly lower (Figure 1D).

In order to assess the differences between patients and controls in an unbiased and genome-wide fashion, we performed principal component analysis (PCA) and hierarchical clustering based on the most variable genes in the data set. This demonstrated that patient and control samples robustly separated from each other (Figure 1E*; Online Supplementary Figure S1A*) and this separation was driven, at least in part, by the expression of monocyte and moDC genes (*Online Supplementary Figure S1B*). Furthermore, the moDC from the youngest (18 months old) and oldest (12 years old) patients with active and non-active disease respectively, clustered closer together compared to the third patient (6 years old, non-active disease). Moreover, none of the three patients was on treatment at sampling, indicating that the separation of patients from controls was not affected by age, disease status or treatment of the patients. Additionally, differential expression analysis on the entire transcriptome revealed thousands of genes to be significantly dysregulated in LCH patient cells (Figure 1F*; Online Supplementary Tables S2* and *S3*). Importantly, the genes differentially expressed in our experiments matched well with those previously described in arrays of lesion-derived LCH cells[20] (*Online Supplementary Figure S1C*). In order to characterize the differentially expressed and top PCA-loaded genes, we analyzed their gene ontology enrichments for processes known to be affected in LCH. This revealed that while immune system processes were both up- and downregulated in LCH-derived *versus* control-derived cells, genes regulating cell-cell adhesion were downregulated and cell cycle genes were upregulated in LCH cells (Figure 1G; *Online Supplementary Figure S1D*).

Stimulation of monocyte-derived dendritic cells with interferon-γ

Recent single-cell sequencing efforts have identified INFγ signaling in LCH cells.[21] Thus, we introduced INFγ stimulation into our moDC differentiation protocol to evaluate its relative effects on the transcriptomes of our patient and control cells (Figure 2A). Confirming the effects of INFγ treatment, hierarchical clustering demonstrated that treated samples generally clustered together when compared to untreated cells from the same individual (*Online Supplementary Figure S2A*). Gene ontology analysis of genes affected by INFγ showed that treated cells downregulated proliferation genes and upregulated those involved in INFγ response and immune cell activation (*Online Supplementary Figure S2B, C*). However, this transcriptional response did not affect the clear separation observed between patient-derived and control-derived moDC by hierarchical clustering (Figure 2B).

Comparison of control and patient moDC treated with INFγ revealed a similar number of differentially expressed genes to that of untreated cells (Figures 1F and 2C; *Online Supplementary Tables S2 and S3*). However, cells from patients showed a more pronounced response to INFγ compared to controls (Figure 2D, E). In order to characterize the biological processes that are differentially affected by INFγ, we performed gene ontology analysis. Like in the case without INFγ treatment, patient cells both up- and downregulated genes involved in immune system processes. In contrast, INFγ increased the enrichment of genes involved in cell migration in control cells over patient cells. In patient cells, INFγ treatment exacerbated the differential expression of genes involved in the MAPK pathway, receptor-mediated endocytosis and regulated exocytosis (Figure 2E, F). Notably, exocytosis terms were found within the top ten most significant gene ontologies upregulated in patient cells (*Online Supplementary Table S3*).

As vesicle trafficking was affected on multiple levels in our RNA-seq data, we looked specifically at the various pathways involved in endocytosis, endosomal sorting and exocytosis.[22,23] This revealed that while caveolin and clathrin were downregulated in patient cells, most scavenger receptors and structural components of endocytosis were upregulated (*Online Supplementary Figure S3*). Moreover, although markers of early endosomes and lysosomes were downregulated in patients, various markers of COP-II-mediated anterograde trafficking, late and recycling endosomes, as well as multivesicular bodies were upregulated in patient cells.[24-26] This was mirrored by an increase in specific syntaxin, synaptogamin and SNARE genes, as well as markers of vesicle fusion and lysosomal exocytosis,[27] which together illustrated the complexity of the LCH exocytosis phenotype (*Online Supplementary Figure S3*).

In order to confirm that the biological processes identified by gene ontology analysis in our *in vitro* system were also active *in vivo* in LCH cells within patient lesions, we turned to a recently published single-cell RNA-seq data set.[21] We used *CD1A* and *CD14* to map where LCH cells and monocytes were located within the cell dispersion maps from each of the seven patient lesions analyzed. In this way, we observed that the MAPK, endocytosis and, particularly, exocytosis genes we found enriched in our patient cells were primarily expressed by monocytes and LCH cells, within patient lesions (Figure 2G; *Online Supplementary Figure S4*).

As our patient samples were limited and heterogeneous,

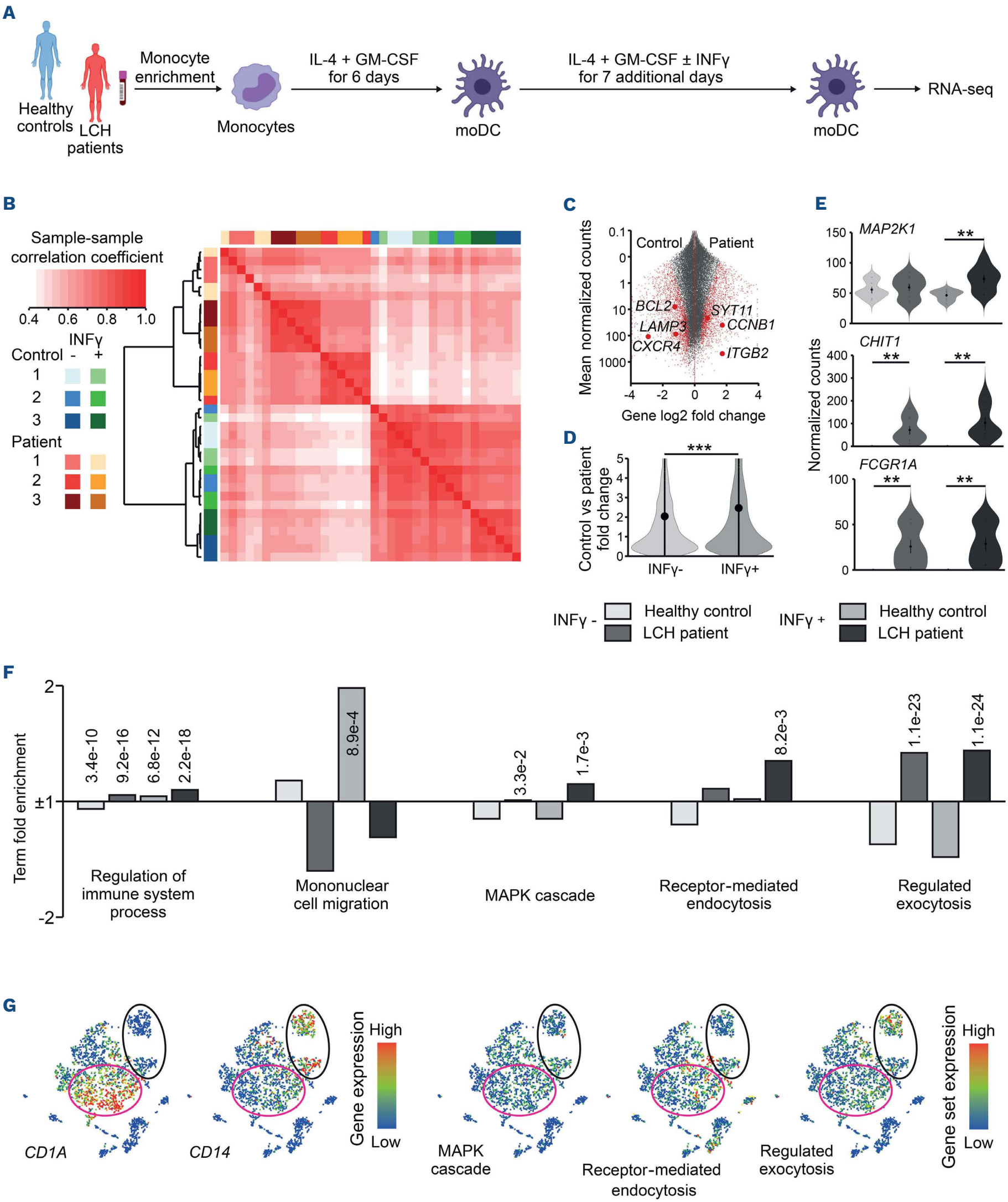

Figure 2. Interferon-γ enhances abnormal Langerhans cell histiocytosis patient monocyte-derived dendritic cell membrane trafficking. (A) Schematic diagram of the differentiation and stimulation protocol applied to monocytes isolated from healthy controls or patients. (B) Hierarchical clustering of sample-sample Pearson correlations for all control and patient monocyte-derived dendritic cells (moDC) ± interferon-γ (INFγ) treatment. (C) Gene expression comparison between control and patient moDC treated with INFγ. Red dots represent genes with significantly different expression. (D) Magnitude of differential gene expression between

Continued on following page.

control and patient moDC when untreated or treated with INFγ. (E) Normalized count data in control and patient moDC ± INFγ treatment for genes exemplifying the gene ontology pathways regulated in (F). (F) Gene ontology term fold enrichments for genes differentially expressed between control and patient moDC ± INFγ treatment. *P* values for significantly enriched terms are inset. (G) Single cell RNA-sequencing data from Halbritter *et al.*[21] showing the expression of markers for Langerhans cell histiocytosis (LCH) cells (*CD1A*, pink circle) and monocytes (*CD14*, black circle), as well as the genes we found differentially expressed within the gene ontology terms listed. Statistics for (D) performed using a two-tailed, unpaired *t*-test and for (E) using the adjusted *P* value from DESeq2. ***P*<0.01 and ****P*<0.001. GM-CSF: granulocyte-macrophage colony-stimulating factor.

we wished to confirm the biological processes dysregulated in LCH moDC by comparing these samples with additional age-matched control groups. Thus, we sequenced moDC from five healthy pediatric controls and three pediatric CD patients (Figure 3A; *Online Supplementary Table S4*). Clustering these samples together with our previous data showed distinct clusters of CD and LCH samples separated from one CD and all control samples (initial and additional pediatric, n=8) (Figure 3B). Performing differential expression analysis between all control samples and either LCH or CD samples revealed more differences between controls and LCH cells (Figures 3C, D). Importantly, the differences in gene expression levels were as significant between LCH moDC and each of the three other sample groups (Figure 3E). Finally, we assessed the potential enrichment of gene ontology terms related to those we found upregulated in our previous analysis. In contrast to their upregulation in LCH moDC, CD moDC downregulated genes involved in MAPK cascade, proliferation, endocytosis and exocytosis, while chemotaxis was instead a feature of these cells (Figure 3F).

Endo- and exocytosis phenotype confirmation

Since gene ontology and pathway analysis suggested that receptor-mediated endocytosis genes were upregulated in LCH cells, we wished to functionally confirm this phenotype in moDC cells from a larger and more homogeneous cohort. To this end, EM analysis of moDC from seven LCH patients and seven control samples revealed dense structures within moDC, which were significantly enriched in LCH cultures (Figure 4A, B). Interestingly, these structures were not observed at all when monocytes were isolated with a different protocol that did not involve incubation with magnetic beads (*Online Supplementary Figure S5*). This suggested that antibody-coated magnetic beads were aberrantly endocytosed during patient monocyte isolation, reflecting the transcriptional changes detected by RNA-seq.

As genes regulating exocytosis pathways were particularly upregulated in LCH cells, it was important to understand how this phenotype manifested itself in LCH. In order to study this, we analyzed the vesicles and soluble proteins present in conditioned media from patient and control moDC cultures. Characterization by EM and nanoparticle tracking analysis revealed an abundance of EV 50-200 nm in size in culture media from both patients and controls (Figure 5A, B). In order to separate and quantify the EV and soluble proteins present in the media, we performed size exclusion chromatography (Figure 5C). This analysis revealed no difference in the amount of soluble proteins present in media from healthy controls and LCH patients, though patient cells treated with INFγ secreted higher protein amounts than untreated patient cells (Figure 5D). Importantly, LCH cells secreted significantly more EV than control cells regardless of their exposure to INFγ, as quantified by nanoparticle tracking. Interestingly, while control cells secreted significantly less EV in the presence of INFγ, LCH patient cells increased the quantity of secreted EV (Figure 5E).

Characterization of the monocyte-derived dendritic cell secretome

Since we consumed all our primary moDC media performing size exclusion, we turned our analysis to moDC derived from an expanded cohort of LCH patients (*Online Supplementary Table S1*) and healthy controls to explore the differences between control and patient secretomes. Analysis of moDC conditioned media using a Luminex panel of selected cytokines known to be secreted by monocytes and DC revealed a significant decrease in the levels of CCL2 released by patients, while all other factors were found at similar levels in the media from patients and controls (*Online Supplementary Figure S6A*). In a parallel attempt to understand the differences between EV secreted by LCH and control moDC, we utilized the MACSplex EV surface protein profiling assay. These experiments revealed lower levels of CD81 and a trend towards higher levels of HLA-DRDPDQ on patient EV, while most other markers were found at similar levels (*Online Supplementary Figure S6B*).

Even though vesicle quantities were clearly increased in patients, the MACSplex assay did not demonstrate clear pathogenic differences between patient and control EV. Therefore, we sought to better understand their functional distinctions. EV are known to carry and deliver diverse protein-, lipid- and nucleic acid cargo between cells and mRNA has attracted particular attention recently due to its role in directly regulating cellular activity.[12] RNA-seq followed by PCA of the most variable genes in the data set showed LCH patient-derived EV transcriptomes to cluster close together, in contrast to control-derived EV, which were more heterogenous (Figure 6A). Furthermore, differential expression analysis revealed hundreds of genes to be specifically enriched in either control or pa-

tient EV (Figure 6B; *Online Supplementary Tables S5* and *S6*). Although it might have been expected that these transcripts simply represented the most highly expressed genes in control and patient cells, this was not the case (*Online Supplementary Figure S7A*). Instead, only LCH-derived EV were specifically enriched for the genes found to be upregulated in the original cohort of patient cells (Figure 6C).

In order to further understand which cellular transcripts were sorted into EV, we performed differential expression

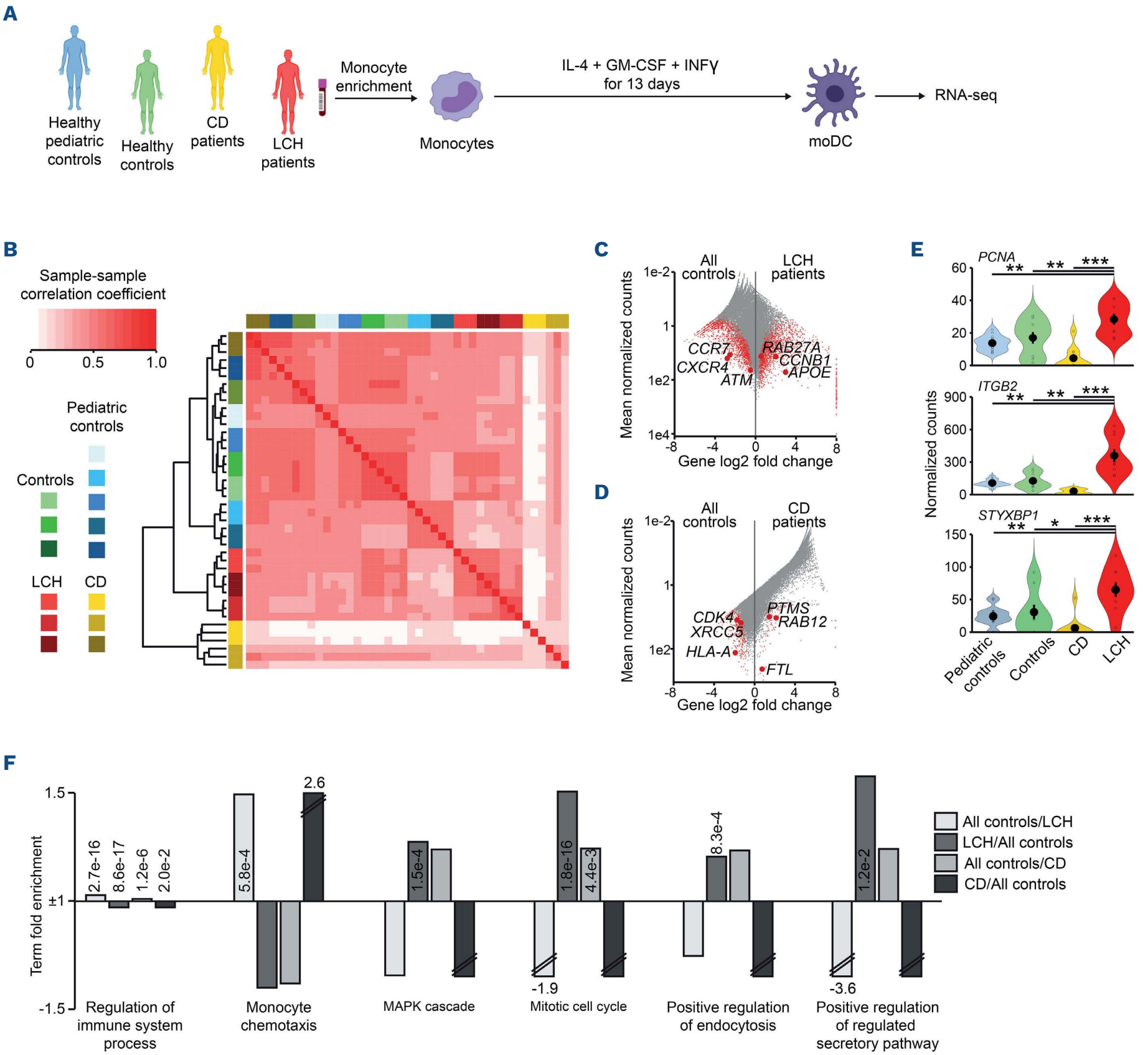

Figure 3. Vesicle trafficking phenotypes are robust and unique to Langerhans cell histiocytosis samples. (A) Schematic diagram of the differentiation and stimulation protocol applied to monocytes isolated from healthy (adult) controls, healthy pediatric controls, Crohn's disease (CD) or Langerhans cell histiocytosis (LCH) patients. (B) Hierarchical clustering of sample-sample Pearson correlations for monocyte-derived dendritic cells (moDC) from the initial cohort of healthy controls and LCH patients and the additional cohort of healthy pediatric controls and CD patients. (C, D) Gene expression comparison between all healthy controls and LCH (C) or CD (D) patient moDC. Red dots represent genes with significantly different expression. (E) Batch corrected normalized count data in original and pediatric controls, as well as CD and LCH patient moDC for genes exemplifying the gene ontology pathways regulated in (F). Statistics performed using unpaired, two-tailed *t*-tests $^{**}P<0.01$ and $^{***}P<0.001$. (F) Gene ontology term fold enrichments for genes differentially expressed between all healthy controls and LCH patient moDC. *P* values for significantly enriched terms are inset. GM-CSF: granulocyte-macrophage colony-stimulating factor.

analysis between cells and EV and plotted their normalized expression values against one another. This showed that EV-enriched genes were expressed at lower levels in patient and control cells relative to the genes enriched in cells (*Online Supplementary Figure S7B-E*). Moreover, the difference between control and patient EV-enriched transcripts was larger than that between the cells themselves (*Online Supplementary Figure S7F*).

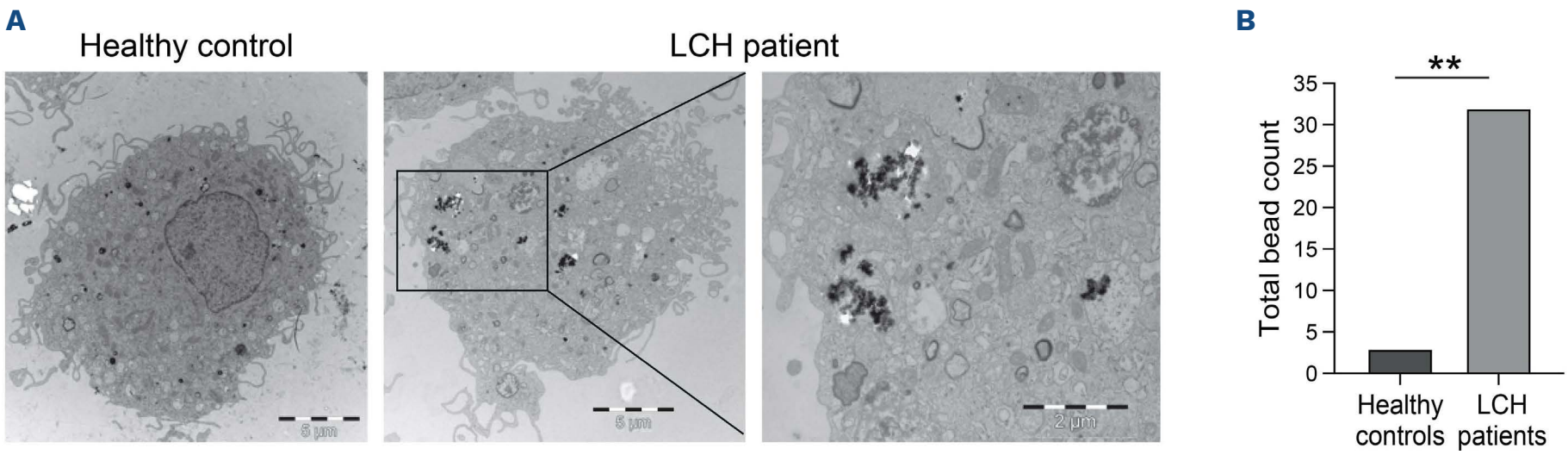

Figure 4. Patient monocyte-derived dendritic cells display abnormal endocytosis. (A) Representative electron micrographs showing beads used in the isolation protocol to be taken up by patient, but not control, monocyte-derived dendritic cells (moDC). Scale bars are inset. (B) Quantification of beads found in moDC from controls (N=7) and patients (N=7). Statistics performed using Mann-Whitney test. ***P*<0.01.

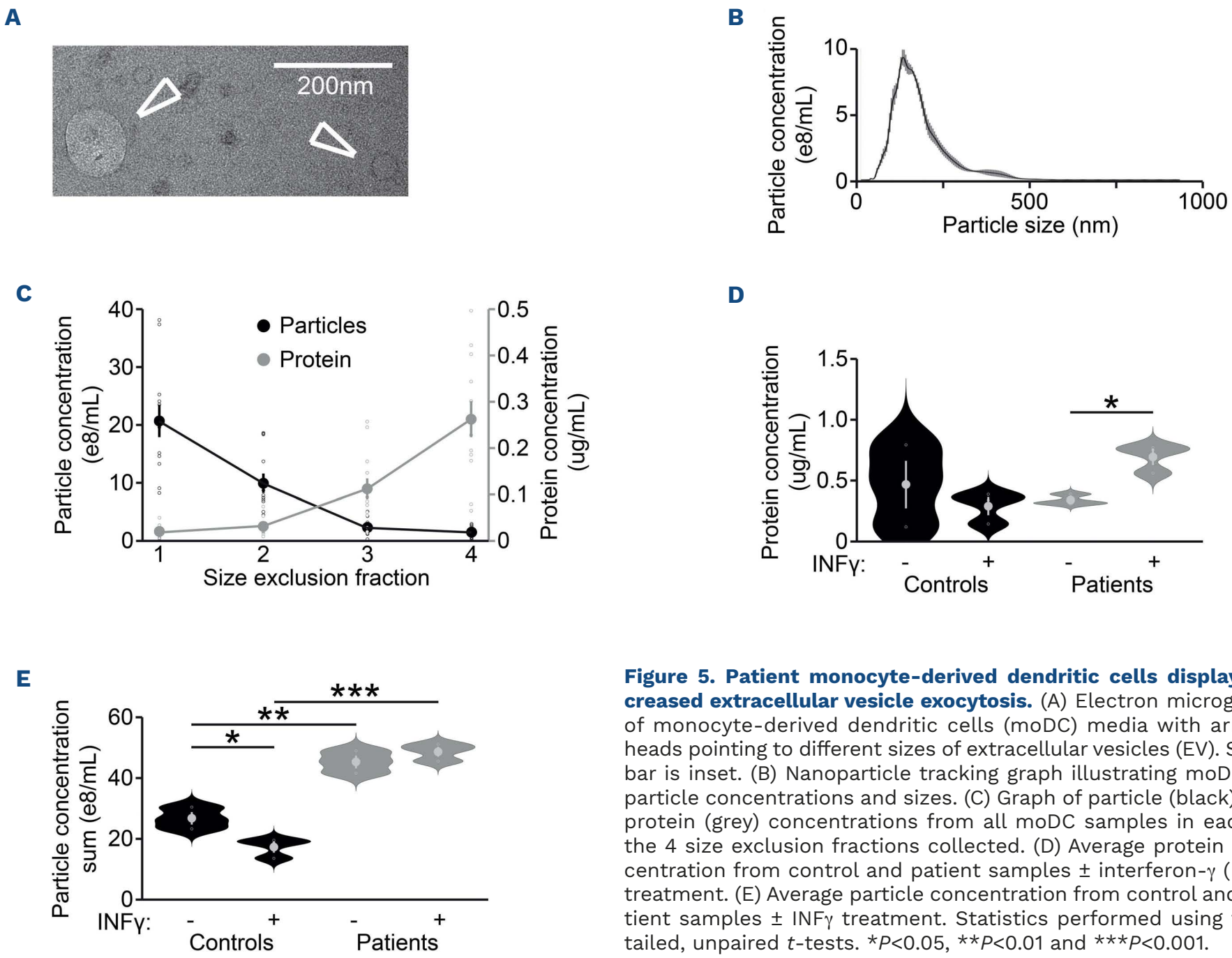

Figure 5. Patient monocyte-derived dendritic cells display increased extracellular vesicle exocytosis. (A) Electron micrograph of monocyte-derived dendritic cells (moDC) media with arrowheads pointing to different sizes of extracellular vesicles (EV). Scale bar is inset. (B) Nanoparticle tracking graph illustrating moDC EV particle concentrations and sizes. (C) Graph of particle (black) and protein (grey) concentrations from all moDC samples in each of the 4 size exclusion fractions collected. (D) Average protein concentration from control and patient samples ± interferon-γ (INFγ) treatment. (E) Average particle concentration from control and patient samples ± INFγ treatment. Statistics performed using two-tailed, unpaired *t*-tests. **P*<0.05, ***P*<0.01 and ****P*<0.001.

In order to characterize the potential function of patient-enriched EV-born transcripts on cells in the lesion, we subjected these to gene ontology analysis. This revealed an enrichment of metabolic genes in both patient and control EV. In contrast, each was enriched in transcripts with opposing effects on cell motility, such that control and patient EV were associated with positive regulators of cell motility and cell-cell adhesion, respectively (Figure

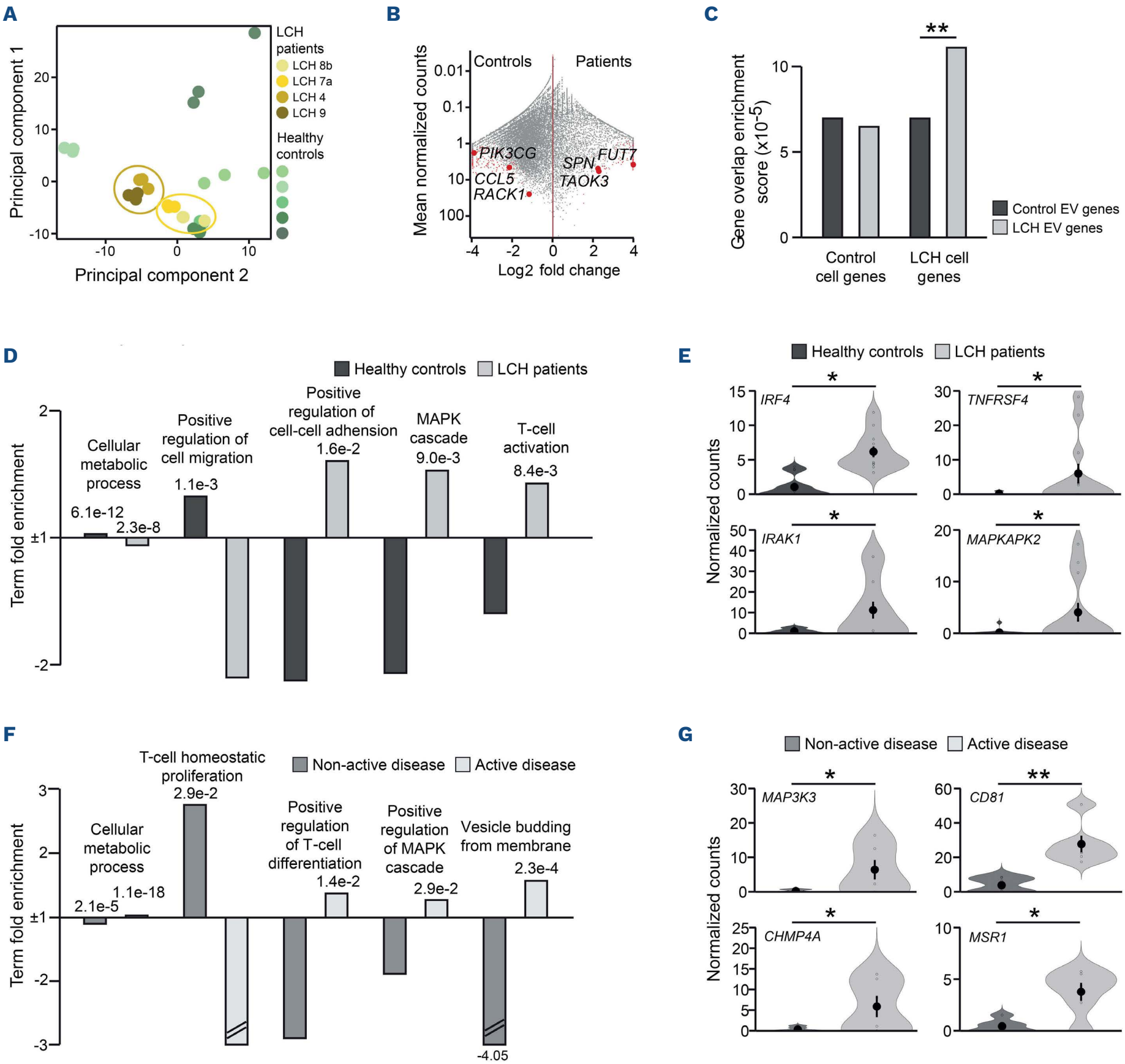

Figure 6. Langerhans cell histiocytosis extracellular vesicles carry transcripts promoting Langerhans cell histiocytosis lesion properties. (A) Principal component analysis of control and patient extracellular vesicle (EV) transcriptomes. (B) Gene expression comparison between EV secreted from INFγ-treated control and patient monocyte-derived dendritic cells (moDC). Red dots are genes with significantly different expression. (C) Overlap enrichment of genes differentially expressed in control and patient moDC cells and EV. Statistics performed using R prcomp. ***P*<0.01. (D) Gene ontology term fold enrichments for genes differentially expressed between INFγ-treated control and patient moDC EV. *P* values for enriched terms are inset. (E) Normalized count data in INFγ-treated patient and control moDC EV for genes exemplifying the gene ontology pathways regulated in (D). (F) Gene ontology term fold enrichments for genes differentially expressed between EV derived from patients with non-active or active Langerhans cell histiocytosis (LCH). *P* values for enriched terms are inset. (G) Normalized count data in EV derived from patients with non-active or active disease for genes exemplifying the gene ontology pathways regulated in (F). *DESeq2 adjusted *P* value <0.05 and **DESeq2 adjusted *P* value <0.01.

6D). Furthermore, a strong enrichment of genes with well-characterized roles in T-cell activation and MAPK cascade was observed specifically in patient cells (Figures 6D, E). Interestingly, patient EV transcriptomes could be clearly separated into two subclusters based on PCA: one derived from patients with active disease and one from patients with non-active disease (Figure 6A; *Online Supplementary Table S1*). By performing differential expression analysis on these two groups (*Online Supplementary Figure S7G*), EV derived from patients with active disease were more enriched in transcripts involved in T-cell differentiation, MAPK signaling and vesicle trafficking than those from patients with non-active disease (Figures 6F, G; *Online Supplementary Table S7*).

Langerhans cell histiocytosis secretome affects the function of lymphocytes

Since gene ontology analysis revealed upregulation of various terms related to lymphocyte function in EV secreted from LCH patient moDC, we sought to investigate how these would affect lymphocytes *in vitro*. For this, we isolated PBMC from buffy coats from three healthy donors and cultured them in the presence of either LCH or control moDC supernatants for 18 hours. Cells were then stained with a 22-color flow cytometry panel (*Online Supplementary Table S8*) to phenotypically characterize the lymphocyte subpopulations in the stimulated PBMC. Single alive lymphocytes from each donor for each stimulation were analyzed with uniform manifold approximation and projection (UMAP) to achieve dimensionality reduction. UMAP analysis (Figure 7A; *Online Supplementary Figure S8A*) showed that the same lymphocyte subsets could be detected in both LCH- and control-treated PBMC. These were $CD4^+$ and $CD8^+$ T cells (including MAIT cells), NK cells and ILC (Figure 7B; *Online Supplementary Figure S8B*). Unsupervised clustering with phenograph subdivided the main lymphocyte subsets into 20 distinct subpopulations based on the median fluorescence intensity of cell markers (Figures 7C, D). Investigation of the frequency of each subset in each donor when treated with LCH or control medium (Figure 7E) revealed that LCH medium significantly decreased the frequencies of Treg (C2), $CD8^+$ activated/regulatory cells (C11) and non-activated NK cells (C1, C5). Moreover, LCH media also resulted in a relative increase in the frequencies of naïve $CD4^+$ T cells (C8), effector memory $CD4^+$ T cells with a naïve phenotype (C7) and mature activated NK cells (C4), while no significant difference was observed in other lymphocyte subsets.

Discussion

One challenge in understanding LCH pathology is that the lesion creates a unique niche of immune cells with complex phenotypes and interactions that cannot be accurately recapitulated in healthy individuals. However, as LCH cells are a type of $CD1a^+$ DC, and monocytes/monocyte-like cells were proposed to contribute to the LCH cell pool,[21,28,29] we felt it would be informative to derive these *in vitro* and apply an unbiased RNA-seq-based approach to study their niche-independent differences. Although the cells analyzed were not *bona fide* LCH cells, this analysis uncovered novel vesicle trafficking phenotypes and confirmed a previously described increase in MAPK activity, impaired DC differentiation and cell migration defects.[20,30,31] These phenotypes agree with previous studies reporting low CCR7 protein levels in LCH cells in lesions and an overall semi-mature mixed monocyte-macrophage-DC phenotype.[20,31-33] This data demonstrated that our differentiation system adequately recapitulated characteristics of *bona fide* LCH cells *in vitro*. INFγ expression has been previously documented in LCH lesions[34,35] and LCH cells are known to express IFNγR1.[35] However, little is known about the impact of INFγ on LCH pathology. Thus, we treated moDC with INFγ and compared their transcriptional profiles with those of unstimulated cells. We found that INFγ treatment exacerbated the increased expression of genes involved in MAPK signaling, endocytosis and exocytosis in LCH patient moDC. Functionally, we found that control moDC decreased their release of EV upon INFγ stimulation, while patient cells increased the secretion of both proteins and EV under these conditions. This supports the interpretation that patient cells are inherently vulnerable to immunological stimuli, possibly explaining the hypercytokinemia detected in patient lesions, blood and CSF.[5-8,36,37]

Our results indicated that increased proliferation, endocytosis and exocytosis are amongst the most pronounced phenotypes in LCH cells, though these have not been previously described in LCH. The finding of multiple exocytosis terms within the top ten most enriched gene ontology terms describing patient moDC demonstrated this importance (*Online Supplementary Table S3*). EV are recognized as having a key role in tumor growth through the reprogramming of tissue resident cells and formation of the tumor niche. Their ability to stimulate angiogenesis, drive matrix remodeling and enable immune escape are well documented in several cancers and thus it is possible that EV have a similar role in LCH pathogenesis. Moreover, their unique capability to cross the blood brain barrier provides a potential lead in the link between LCH and pediatric neurodegeneration.[38-40] Unfortunately, the small size of our cohort constitutes a limitation of our study and the modest number of moDC obtained prevented us from performing all experiments on the same samples. Regardless, we confirmed the LCH transcriptional phenotypes that we discovered by comparing to three different control groups, including another inflammatory granuloma disease, and functionally verified them using EM, nanoparticle tracking and lymphocyte stimulation assays.

Moreover, the biological relevance of our findings was supported by our ability to map the expression of the dysregulated gene sets in LCH moDC to the *CD1A* and *CD14* expressing cells in LCH lesions.[21]

Although the mechanisms that underpin LCH have remained elusive, our understanding of the intrinsic pathways dysregulated in LCH cells was improved by the discovery of MAPK pathway mutations in LCH cells. Interestingly, MAPK signaling influences vesicle trafficking, which may lead to the increased exocytosis we observed. As EV can deliver a broad range of biological cargo to influence neighboring cells,[12,13] they represent both a novel pathological mechanism and a potential source of disease biomarkers. Indeed, the analysis of EV contents in plasma and other biofluids have been proposed as tumor biomarkers in various cancers.[13] Thus, EV secreted by cells found in LCH granulomas could possibly be used both as early LCH diagnostic markers and as markers for disease state and therapy evaluation.

The upregulation of genes such as *LAMTOR2* and components of the ESCRT machinery in LCH moDC hinted at previously underappreciated pathological mechanisms. LAMTOR2 resides mainly in late endosomes, where it regulates vesicle sorting and has been shown to be necessary for Langerhans cell proliferation and survival by regulating ERK and mTORC signaling.[25] Interestingly, inhibition of mTOR was sufficient to reduce production of inflammatory cyto-

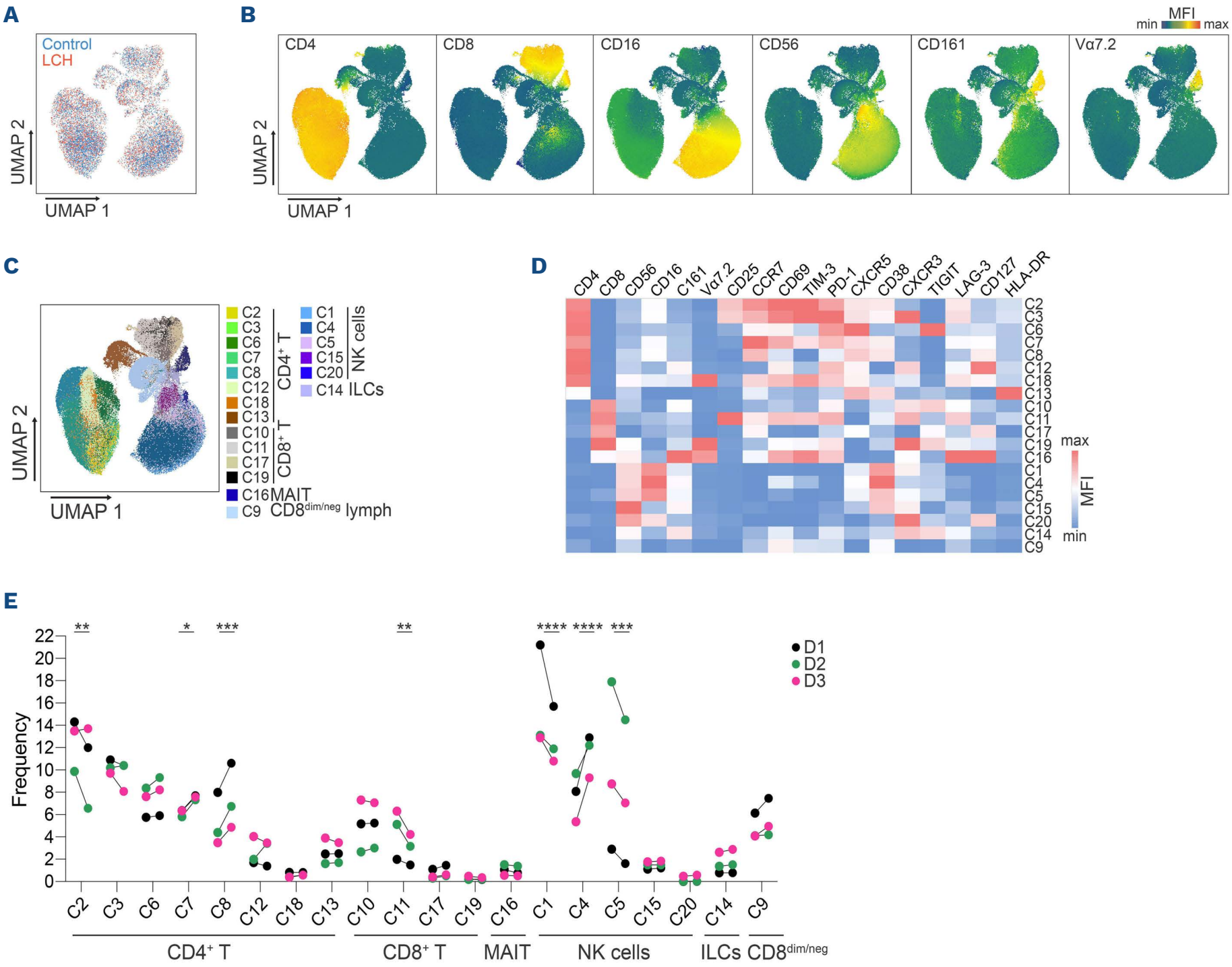

Figure 7. Langerhans cell histiocytosis secretome reprograms lymphocyte function. (A) Uniform manifold approximation and projection (UMAP) on concatenated files of 114,000 lymphocytes from 3 healthy donors (38,000 cells each) treated either with control conditioned culture medium (light blue) or 114,000 lymphocytes from the same 3 healthy donors (38,000 cells each) treated with Langerhans cell histiocytosis (LCH) conditioned culture medium (red). (B) UMAP displaying the median fluorescence intensity (MFI) of the indicated markers. (C) Distribution of the 20 identified phenograph clusters overlaid on the UMAP projection. (D) MFI of each marker in the phenograph clusters. (E) Frequency of each cluster in each donor when treated with CN medium (first point) or LCH medium (second point), linked with a line. Statistics in (E) performed using Multiple paired *t*-tests. **P*<0.05, ***P*<0.01, ****P*<0.001 and *****P* <0.0001.

kines by *BRAF* V600E^{+} hematopoietic progenitors and improve outcomes in treated mice.[41] Moreover, the ESCRT machinery plays a vital role in the cellular processes essential for exosome release and its activation would contribute to the increased exocytosis characterizing LCH cells.[42] The perturbed vesicle trafficking resulting from the dysregulation of these genes may explain why we found patient moDC EV to be particularly enriched in transcripts involved in T-cell activation, cell adhesion and MAPK signaling. Importantly, the lateral transfer of these phenotypes would help justify the behavior of lesional cells, including the observation of activated T cells in the absence of stimulatory cytokines.[43] In order to assay this directly, we tested the effects of patient and control moDC conditioned media on lymphocyte activity. Interestingly, this revealed a reduction in the frequency of activated T cells and inactive NK cells, and a striking increase in the frequency of naïve T cells and activated NK cells. However, given that the activation markers in these cell types overlap extensively, and NK terms are very limited in the gene ontology database, it is not surprising that T-cell regulation was highlighted in our data. Regardless, this constitutes the first example of histiocytosis cells reprograming other cells in their niche, which is a common function of EV in other neoplastic diseases.[41]

Together, our findings indicate that LCH patient cells are intrinsically sensitive to immune insult, reveal important mechanisms of disease pathology, and suggest EV as potentially valuable target in LCH patient diagnostics and therapy. For example, a prospective study of LCH patient EV in liquid biopsies has the potential to reveal biomarkers such as mutational status, which could improve the sensitivity of LCH diagnosis and treatment monitoring. Moreover, if EV are confirmed as a pathogenic mechanism of LCH, then sequestering them in lesions or inhibiting their production may prove a potent therapeutic approach, as has been recently demonstrated in systemic inflammation and melanoma.[44-46]

Disclosures

AG and SEA are consultants for and have equity interests in Evox Therapeutics Ltd., Oxford, UK. JIH served as consultant for SOBI. All the other authors have no conflicts of interest to disclose.

Contributions

DWH and ML developed the concept and methodology of the study. DWH, MA, AG, JJ, NH and ML performed the investigation. DWH, EK, AG and ML analyzed data. TvBG, CB, SOÅ, TH-H, HA and J-IH recruited patients and provided clinical information. DWH, KD, MS, SEA, J-IH and ML provided resources. ML supervised the study. DWH and ML prepared the figures and wrote the manuscript. All authors reviewed and approved the final version of the manuscript.

Acknowledgments

The authors would like to thank all patients and unrelated volunteers (controls) who agreed to participate in the study, all clinicians and nurses involved in collection of blood samples and the Single Cell Core Facility in Karolinska Institute Flemingsberg. We would also like to thank Kjell Hultenby and Eva Blomén from the electron microscopy unit (EMil) at Karolinska Institute Flemingsberg for their valuable assistance with the EM experiments.

Funding

The study was supported by grants to DWH from the Swedish Childhood Cancer Fund, Ishizu Matsumurais Donation and OEE Johanssons Foundation, to JIH from the Swedish Childhood Cancer Fund, the Swedish Cancer Society, the Swedish Cancer and Allergy Fund, and Region Stockholm (ALF-project) and to ML from the Swedish Childhood Cancer Fund, Karolinska Institute, Dr Åke Olsson Foundation for hematological research, Fredrik O Ingrid Thurings Foundation, Mary Béve Foundation for pediatric cancer research and Märta and Gunnar V Philipsons Foundation.

Data-sharing statement

All data needed to evaluate the conclusions of the paper are presented in the paper or in the Online Supplementary Appendix without providing personally identifiable information.

References

1. Allen CE, Merad M, McClain KL. Langerhans-cell histiocytosis. N Engl J Med. 2018;379(9):856-868.
2. Badalian-Very G, Vergilio JA, Degar BA, et al. Recurrent BRAF mutations in Langerhans cell histiocytosis. Blood. 2010;116(11):1919-1923.
3. Sahm F, Capper D, Preusser M, et al. BRAFV600E mutant protein is expressed in cells of variable maturation in Langerhans cell histiocytosis. Blood. 2012;120(12):e28-34.
4. Zeng K, Wang Z, Ohshima K, et al. BRAF V600E mutation correlates with suppressive tumor immune microenvironment and reduced disease-free survival in Langerhans cell histiocytosis. Oncoimmunology. 2016;5(7):e1185582.
5. Lourda M, Olsson-Akefeldt S, Gavhed D, et al. Detection of IL-17A-producing peripheral blood monocytes in Langerhans cell histiocytosis patients. Clin Immunol. 2014;153(1):112-122.
6. Oh Y, Morimoto A, Shioda Y, et al. High serum osteopontin levels in pediatric patients with high risk Langerhans cell histiocytosis. Cytokine. 2014;70(2):194-197.
7. Lourda M, Olsson-Akefeldt S, Gavhed D, et al. Adsorptive depletion of blood monocytes reduces the levels of circulating interleukin-17A in Langerhans cell histiocytosis. Blood. 2016;128(9):1302-1305.
8. Morimoto A, Oh Y, Nakamura S, et al. Inflammatory serum cytokines and chemokines increase associated with the disease

extent in pediatric Langerhans cell histiocytosis. Cytokine. 2017;97:73-79.
9. Andersson By U, Tani E, Andersson U, Henter JI. Tumor necrosis factor, interleukin 11, and leukemia inhibitory factor produced by Langerhans cells in Langerhans cell histiocytosis. J Pediatr Hematol Oncol. 2004;26(11):706-711.
10. Kannourakis G, Abbas A. The role of cytokines in the pathogenesis of Langerhans cell histiocytosis. Br J Cancer Suppl. 1994;23:S37-40.
11. van Niel G, D'Angelo G, Raposo G. Shedding light on the cell biology of extracellular vesicles. Nat Rev Mol Cell Biol.2018;19(4):213-228.
12. Elsharkasy OM, Nordin JZ, Hagey DW, et al. Extracellular vesicles as drug delivery systems: why and how? Adv Drug Deliv Rev. 2020;159:332-343.
13. Xu R, Rai A, Chen M, et al. Extracellular vesicles in cancer - implications for future improvements in cancer care. Nat Rev Clin Oncol. 2018;15(10):617-638.
14. Coury F, Annels N, Rivollier A, et al. Langerhans cell histiocytosis reveals a new IL-17A-dependent pathway of dendritic cell fusion. Nat Med. 2008;14(1):81-87.
15. Bost JP, Saher O, Hagey D, et al. Growth media conditions influence the secretion route and release levels of engineered extracellular vesicles. Adv Healthc Mater. 2022;11(5):e2101658.
16. Hagey DW, Kordes M, Gorgens A, et al. Extracellular vesicles are the primary source of blood-borne tumour-derived mutant KRAS DNA early in pancreatic cancer. J Extracell Vesicles. 2021;10(12):e12142.
17. Olsson Akefeldt S, Maisse C, Belot A, et al. Chemoresistance of human monocyte-derived dendritic cells is regulated by IL-17A. PLoS One. 2013;8(2):e56865.
18. Tang-Huau TL, Segura E. Human in vivo-differentiated monocyte-derived dendritic cells. Semin Cell Dev Biol. 2019;86:44-49.
19. Holter W, Ressmann G, Grois N, et al. Normal monocyte-derived dendritic cell function in patients with Langerhans-cell-histiocytosis. Med Pediatr Oncol. 2002;39(3):181-186.
20. Allen CE, Li L, Peters TL, et al. Cell-specific gene expression in Langerhans cell histiocytosis lesions reveals a distinct profile compared with epidermal Langerhans cells. J Immunol. 2010;184(8):4557-4567.
21. Halbritter F, Farlik M, Schwentner R, et al. Epigenomics and single-cell sequencing define a developmental hierarchy in Langerhans cell histiocytosis. Cancer Discov. 2019;9(10):1406-1421.
22. Kaksonen M, Roux A. Mechanisms of clathrin-mediated endocytosis. Nat Rev Mol Cell Biol. 2018;19(5):313-326.
23. Johansen J, Alfaro G, Beh CT. Polarized exocytosis induces compensatory endocytosis by Sec4p-regulated cortical actin polymerization. PLoS Biol. 2016;14(8):e1002534.
24. Jensen D, Schekman R. COPII-mediated vesicle formation at a glance. J Cell Sci. 2011;124(Pt 1):1-4.
25. Sparber F, Scheffler JM, Amberg N, et al. The late endosomal adaptor molecule p14 (LAMTOR2) represents a novel regulator of Langerhans cell homeostasis. Blood. 2014;123(2):217-227.
26. Villasenor R, Kalaidzidis Y, Zerial M. Signal processing by the endosomal system. Curr Opin Cell Biol. 2016;39:53-60.
27. Bonifacino JS, Glick BS. The mechanisms of vesicle budding and fusion. Cell. 2004;116(2):153-166.
28. Hutter C, Kauer M, Simonitsch-Klupp I, et al. Notch is active in Langerhans cell histiocytosis and confers pathognomonic features on dendritic cells. Blood. 2012;120(26):5199-5208.
29. Milne P, Bigley V, Bacon CM, et al. Hematopoietic origin of Langerhans cell histiocytosis and Erdheim-Chester disease in adults. Blood. 2017;130(2):167-175.
30. Shi H, He H, Cui L, et al. Transcriptomic landscape of circulating mononuclear phagocytes in Langerhans cell histiocytosis at the single-cell level. Blood. 2021;138(14):1237-1248.
31. Hogstad B, Berres ML, Chakraborty R, et al. RAF/MEK/extracellular signal-related kinase pathway suppresses dendritic cell migration and traps dendritic cells in Langerhans cell histiocytosis lesions. J Exp Med. 2018;215(1):319-336.
32. Annels NE, Da Costa CE, Prins FA, et al. Aberrant chemokine receptor expression and chemokine production by Langerhans cells underlies the pathogenesis of Langerhans cell histiocytosis. J Exp Med. 2003;197(10):1385-1390.
33. Senechal B, Elain G, Jeziorski E, et al. Expansion of regulatory T cells in patients with Langerhans cell histiocytosis. PLoS Med. 2007;4(8):e253.
34. Egeler RM, Favara BE, van Meurs M, Laman JD, Claassen E. Differential In situ cytokine profiles of Langerhans-like cells and T cells in Langerhans cell histiocytosis: abundant expression of cytokines relevant to disease and treatment. Blood. 1999;94(12):4195-4201.
35. Quispel WT, Stegehuis-Kamp JA, Santos SJ, et al. Intact IFN-gammaR1 expression and function distinguishes Langerhans cell histiocytosis from mendelian susceptibility to mycobacterial disease. J Clin Immunol. 2014;34(1):84-93.
36. Ismail MB, Akefeldt SO, Lourda M, et al. High levels of plasma interleukin-17A are associated with severe neurological sequelae in Langerhans cell histiocytosis. Cytokine. 2020;126:154877.
37. McClain KL, Picarsic J, Chakraborty R, et al. CNS Langerhans cell histiocytosis: common hematopoietic origin for LCH-associated neurodegeneration and mass lesions. Cancer. 2018;124(12):2607-2620.
38. Javadi J, Gorgens A, Vanky H, et al. Diagnostic and prognostic utility of the extracellular vesicles subpopulations present in pleural effusion. Biomolecules. 2021;11(11):1606.
39. Peinado H, Zhang H, Matei IR, et al. Pre-metastatic niches: organ-specific homes for metastases. Nat Rev Cancer. 2017;17(5):302-317.
40. El-Andaloussi S, Mager I, Breakefield XO, Wood MJ. Extracellular vesicles: biology and emerging therapeutic opportunities. Nat Rev Drug Discov. 2013;12(5):347-357.
41. Bigenwald C, Le Berichel J, Wilk CM, et al. BRAF(V600E)-induced senescence drives Langerhans cell histiocytosis pathophysiology. Nat Med. 2021;27(5):851-861.
42. Kim SW, Kim DH, Park KS, et al. Palmitoylation controls trafficking of the intracellular Ca(2+) channel MCOLN3/TRPML3 to regulate autophagy. Autophagy. 2019;15(2):327-340.
43. Quispel WT, Stegehuis-Kamp JA, Santos SJ, Egeler RM, van Halteren AG. Activated conventional T-cells are present in Langerhans cell histiocytosis lesions despite the presence of immune suppressive cytokines. J Interferon Cytokine Res. 2015;35(10):831-839.
44. Gupta D, Wiklander OPB, Gorgens A, et al. Amelioration of systemic inflammation via the display of two different decoy protein receptors on extracellular vesicles. Nat Biomed Eng. 2021;5(9):1084-1098.
45. Chen G, Huang AC, Zhang W, et al. Exosomal PD-L1 contributes to immunosuppression and is associated with anti-PD-1 response. Nature. 2018;560(7718):382-386.
46. Serrati S, Guida M, Di Fonte R, et al. Circulating extracellular vesicles expressing PD1 and PD-L1 predict response and mediate resistance to checkpoint inhibitors immunotherapy in metastatic melanoma. Mol Cancer. 2022;21(1):20.